

Rapid phase imaging with 3D echo-planar imaging (EPI) for quantitative MRI – A simulation study on image artifacts

Paul Polak¹, Robert Zivadinov^{1,2}, and Ferdinand Schweser^{1,2}

¹Department of Neurology, Buffalo Neuroimaging Analysis Center, State University of New York at Buffalo, Buffalo, NY, United States, ²Molecular and Translational Imaging Center, MRI Center, Clinical and Translational Research Center, Buffalo, NY, United States

TARGET AUDIENCE – Researchers interested in rapid imaging and quantitative phase MRI.

PURPOSE – Gradient echo (GRE) imaging has recently received increased attention because the GRE signal carries important information about magnetic tissue properties¹ and microscopic tissue architecture². One of the emerging GRE-based techniques is Quantitative Susceptibility Mapping (QSM), which converts the phase component of the complex-valued GRE signal into a map of the underlying source distribution of magnetic susceptibility¹. However, clinical translation as well as full exploration of the tissue information contained in the signal is seriously hampered by the relatively lengthy acquisition time of GRE imaging. It has recently been proposed to use segmented multi-shot 3D echo-planar imaging (3D EPI) sequences^{3,4,5} to accelerate GRE imaging, as this technique allows acquiring whole brain GRE data with an isotropic nominal resolution of 0.55mm in less than 2 minutes^{3,4,5}.

The relatively long echo train of EPI, which is in the order of tens of milliseconds, gives rise to the question how accurate resulting phase and magnitude images are, and what effect potential inaccuracies have if the images are then used as an input for subsequent quantitative imaging techniques such as QSM. During the EPI readout both magnitude and phase change, potentially resulting in artifacts. In this work we systematically investigate the effect of magnitude signal decay and phase evolution during the readout on the accuracy of complex-valued GRE signals measured with simulated segmented 3D EPI sequences.

METHODS – *Numerical model:* To minimize measurement-related artifacts⁶ and to be able to simulate the complex-valued free-induction-decay (FID) at arbitrary echo times (TE) we decided to base our study on a dedicated realistic numerical brain FID model. This model was created from volunteer brain data acquired with a conventional 3D fly-back multi-echo GRE sequence (8 echoes, TE₁=4ms, ΔTE=4.2ms, TR/FA=38ms/15°, BW=514Hz/px, 75% FOV, 0.84x0.84x1.5mm³ voxel size, matrix 256x192x88) on a 3T scanner (Tim Trio, Siemens Medical Solutions, Erlangen). We combined single-channel images⁷ and calculated the effective transverse relaxation rate R₂^{*} and the PD/T₁-weighted image contrast S₀ (extrapolated to TE=0) from the magnitude decay using logarithmic calculus. The Larmor frequency ω_L in the brain was obtained from the temporal evolution⁹ of unwrapped phase images¹. The resulting maps (R₂^{*}, S₀, and ω_L) were used to simulate the FID signal, S(TE), at different TE_s according to the following relation S(TE) = S₀exp(-R₂^{*}·TE + i·ω_L·TE). *Simulation of the EPI readout:* We simulated the EPI readout process by calculating the effective echo time TE_{line} for each line of the EPI readout train and then the corresponding S(TE_{line}). The raw MRI signal corresponding to each line of the EPI readout was obtained by taking the corresponding Fourier coefficients from the k-space spectrum of S(TE_{line}). Our simulation relies on the simplistic assumption that all decay and phase evolution occur only in the time between the readouts (during the phase steppers); the phase steppers themselves requiring an infinitely short time. In other words, this simplification neglects the signal change during the readout time interval but incorporates the temporal change of the k-space between different lines – each readout line “sees” a different but static S(TE_{line}), which, incidentally, is precisely the assumption conventional multi-echo GRE acquisitions rely on. We simulated EPI acquisitions with varying readout bandwidths (BW_s) and differing numbers of EPI segments, but the readout was always left-to-right and the effective TE (TE_{eff}) was 29ms, i.e. the center of k-space was acquired 29ms after the RF pulse. This echo time was also used in Refs. 3 and 4 for EPI-based phase imaging and QSM. To investigate the impact of the EPI trajectory, or number of segmentations, and the readout bandwidth (BW), we varied the number of lines per excitation between 1 (conventional GRE) and 116 in steps of 2 and the time required for each readout line (the inverse of the readout BW per pixel) between 500μs and 4ms in steps of 250μs. Noise effects were not modeled. *Analysis:* EPI images were compared to the conventional GRE model dataset at 29 ms, S(29ms), which is shown in Figure 1. To allow direct comparison of EPI and conventional GRE by means of difference images, distortions of the EPI images related to the long readout train and the substantial field inhomogeneity in the brain (see Figure 1) were compensated for by registering the EPI images to the conventional GRE images using Advanced Normalization Tools (ANTs)⁹. The root mean square error (RMSE) of registered phase and magnitude images were assessed inside a binary brain mask that was eroded by 5 voxels. The phase RMSE was assessed by complex division of the registered EPI and the model dataset. RMSE values were normalized by the number of voxels used for their calculation.

RESULTS – Figure 2 shows the RMSEs of magnitude and phase as functions of the number of lines per excitation and the readout time per line (inverse BW). The magnitude error (left) increased with the readout time per line (decreasing BW). While the same behavior was also found for the phase error (right), the phase error also depended on the number of lines per excitation, with increasing error for increasing number of lines. Figure 3 shows the magnitude and phase error patterns for three exemplary settings with 14 lines per excitation (used in Refs. 3 and 4): 4ms/line (worst setting; 250Hz/px); 2ms/line (typical setting; used in Refs. 3 and 4; 500Hz/px); 1ms/line (improved setting; 1000Hz/px). All three settings resulted in considerable artifacts on both the magnitude and the phase images. While magnitude images suffer mostly from edge artifacts and low frequency inhomogeneities, phase images show considerable anatomical contrast, particularly in cortical regions. Artifacts were considerably reduced in the improved configuration (right), but were still present (see arrows in Figure 3).

DISCUSSION – Our results indicate that recently reported parameters for high-resolution 3D multi-shot EPI^{3,4} result in substantial artifacts on phase images. Since these artifacts are mainly located at tissue interfaces/edges it can be assumed that their impact is negligible if phase is used for the calculation and analysis of susceptibility in highly iron-laden regions, such as basal ganglia nuclei. However, the results also indicate that the use of EPI may be problematic when susceptibility maps with very high accuracy are required or when more subtle phase contrast is to be investigated, such as microstructural phase in white matter² or cortical phase contrast. The found artifacts are in addition to the known image distortions caused by EPI sequences, e.g., due to eddy currents. Our results show that increasing the number of segments (decreasing the number of lines per excitation) and/or the readout BW (reducing the time per line) diminishes artifacts, if EPI eddy-current distortion effects from a higher readout BW are ignored. While this increases the demand for high-performance gradient systems, both changes also increase the measurement time diminishing the benefit of EPI-based imaging over conventional GRE imaging. Increasing the BW by a factor of N allows a slightly reduced TR, and thus measurement time, but also results in decreased SNR, requiring an increase in the number of averages by a factor of N² to compensate.

CONCLUSION – 3D segmented EPI imaging suffers from subtle but significant artifacts in phase and magnitude images, limiting its application for advanced phase imaging techniques.

REFERENCES – [1] Schweser F, 2011. NeuroImage, 54(4), 2789–2807. [2] Sukstanskii AL and Yablonskiy DA, 2014. Magn Reson Med, 71(1), 345–53. [3] Langkammer C et al, 2014. 3rd QSM Workshop. [4] Sati P et al., 2014. Mult Scler. (epub). [5] Poser BA et al., 2010. NeuroImage, 51(1), 261–6. [6] Feinberg DA and Oshio K, 1994. Magn Reson Med, 32(4), 535–539. [7] Robinson SP et al., 2011. Magn Reson Med, 65(6). [8] Wu B et al., 2012. NeuroImage, 59(1), 297–305. [9] Avants B et al., 2011. NeuroImage. 54:2033-044.

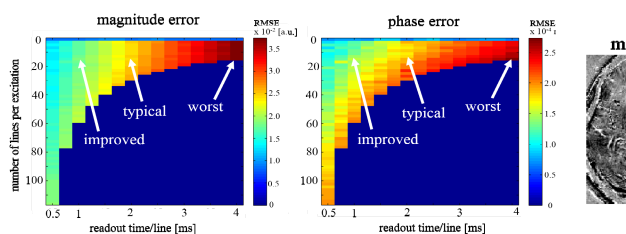


FIGURE 2. Magnitude (left) and phase (right) error (RMSE) as a function of the number of lines per excitation (ordinate) and the readout time per line (abscissa). The dark blue area represents impossible configurations for the chosen TE_{eff} of 29ms. Arrows mark the settings illustrated in Figure 3.

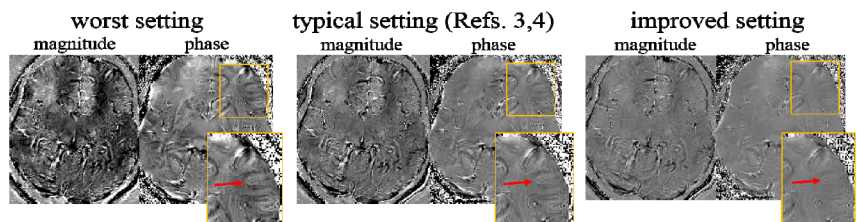


FIGURE 3. Deviation of the simulated EPI data from the conventional GRE model for different settings as marked in Figure 2. Shown are different EPI simulation images of the same slice as shown in Figure 1. Magnitude contrast is [-50,50] a.u., phase contrast is [-0.5,0.5] radians. Insert images are enlarged sections of the region outlined by the yellow box, the red arrow marks cortical contrast.